

Intra-Landau-level collective excitations in a bilayer disordered electronic system

Samvel M. Badalyan* and Chang Sub Kim†

Department of Physics and Institute for Condensed Matter Theory, Chonnam National University, Gwangju 500-757, Korea

(Received 28 June 2004; revised manuscript received 3 January 2005; published 20 April 2005)

We investigate intra-Landau-level collective excitations in a bilayer disordered two-dimensional electron system exposed to a perpendicular magnetic field. The energy spectrum is calculated within the random phase approximation by taking into account the electron-impurity scattering in the self-consistent Born approximation which includes consistent vertex corrections. It is shown that the whole spectrum lies in the finite-wave-vector domain and that there exist multiple wave-vector gaps in the weak Landau-level coupling regime. The signatures of the obtained bilayer excitations in drag and collective excitation measurements are identified.

DOI: 10.1103/PhysRevB.71.153308

PACS number(s): 73.20.Mf, 73.21.-b, 78.30.-j

In bilayer two-dimensional electron systems (2DES), an additional degree of freedom, associated with the layer index, produces collective excitations (CE), which have no counterpart in the individual 2DES.¹ New interlayer electron correlations arise which govern different ferromagnetic and antiferromagnetic phases of the quantum Hall states.² The bilayer CE also play an essential role in the dynamical screening of interlayer Coulomb interactions in the frictional drag effect both in zero³⁻⁵ and finite magnetic fields.^{4,6-9}

The basic source of physical information on the fundamental properties of a system is the spectrum of CE. In a zero magnetic field, the spectrum of CE in the bilayer disorder-free 2DES has been studied comprehensively both in theory¹⁰ and experiment.¹¹ The spectrum includes not only the optical wave with in-phase density fluctuations and the usual square-root dispersion, but also an additional acoustical branch with out-of-phase fluctuations and a linear dispersion. In the finite magnetic fields, the dispersion of inter-Landau-level (LL) CE with energies close to the multiples of the cyclotron energy was obtained analytically at the zero temperature limit.¹² Experimental measurements of the spectrum of inter-LL CE in bilayer 2DES were performed only recently; the principal Bernstein magnetoplasmon modes were observed by means of inelastic light scattering.¹³

Of central importance, however, is the spectrum of CE in the extreme quantum limit when no kinetic energy change occurs in the 2DES. These CE with energies, $\hbar\omega$, below the cyclotron energy, $\hbar\omega_B$, are referred to as the intra-LL CE. In the fractional quantum Hall effect (FQHE) regime the intra-LL CE are the well known magnetorotons in single-layer¹⁴ and double-layer¹⁵ 2DES, with the dispersion minima at wave vectors $q \sim 1/\ell_B$,¹⁶ where ℓ_B is the magnetic length. In disordered 2DES, a continuum of particle-hole excitations takes place within a broadened LL. In the individual, disordered 2DES the spectrum of intra-LL CE has been studied by Antoniou *et al.*¹⁷ for the lowest LL, and it has been found that the plasmonlike CE emerge above the particle-hole continuum (PHC). It has also been predicted by Merkt¹⁸ that in the disordered 2DES, electron-electron (e-e) interaction overcomes Kohn's theorem¹⁹ and results in a low-lying, disorder-induced, cyclotron-resonance mode. Recently, the importance of intra-LL CE in the drag effect has been also discussed.⁸

This paper reports theoretically on the spectrum of

intra-LL CE in the bilayer disordered 2DES in a perpendicular magnetic field at finite temperatures when a higher LL is partially filled. We treat e-e interaction within the random phase approximation (RPA) and electron-impurity (e-i) scattering in the self-consistent Born approximation (SCBA),²⁰ which includes the consistent vertex corrections to the response function of the individual 2DES.¹⁷ We obtain that the whole spectrum of intra-LL CE is located in a finite-wave-vector interval, and, depending on the system parameters, there can exist l_0 forbidden zones within this wave-vector interval. (l_0 is the Landau index of the outermost partially filled LL.) The reason why there exist such wave-vector gaps is because the 2DES become unable to respond in the wave-vector zones where the e-e interaction vanishes effectively. The intra-LL CE emerge above the PHC only at sufficiently large values of mobility, and, despite the fact that the filling factor is large in the regime of our interest, the LL broadening and temperature are chosen to be much smaller than the cyclotron energy so that the LL mixing is weak. We include this weak LL mixing effect in our calculation and establish that the spectrum exhibits the wave-vector gaps in the studied regime.

The bilayer dielectric tensor $\varepsilon_{ij}(q, \omega)$ ($i, j=1, 2$ are the layer indices) is given in terms of the irreducible electron polarization function $\Pi_{ij}(q, \omega)$, which is obtained from the solution of a matrix Dyson equation for the dynamically screened Coulomb interaction $\hat{V}(q, \omega)$. It has the following usual form:

$$\hat{V}(q, \omega) = \hat{v}(q)[1 - \hat{v}(q)\hat{\Pi}(q, \omega)]^{-1} \equiv \hat{v}(q)\hat{\varepsilon}^{-1}(q, \omega), \quad (1)$$

where all quantities are 2×2 matrices, and \hat{v} denotes the bare Coulomb interaction tensor. For simplicity we assume that the layers are infinitely thin and use $v_{11}=v_{22}=v=2\pi e^2/\kappa_0 q$ and $v_{12}=v_{21}=\exp(-q\Lambda)v$, where κ_0 is the static dielectric constant, and Λ is the interlayer spacing. We neglect tunneling between the layers and adopt an approximation where the interlayer polarization functions are zero, $\Pi_{12}=\Pi_{21}=0$. Then, the components of the inverse dielectric tensor are given as $\varepsilon_{11,22}^{-1}(q, \omega)=\varepsilon_{2,1}(q, \omega)/\varepsilon_{bi}(q, \omega)$

and $\varepsilon_{12,21}^{-1}(q, \omega) = v_{12}(q, \omega) / \varepsilon_{\text{bi}}(q, \omega)$. Here, $\varepsilon_{1,2}(q, \omega) = 1 - v_{11}\Pi_{11,22}(q, \omega)$ and $\Pi_{11,22}(q, \omega)$ are the screening and polarization functions in each layer. The bilayer screening function $\varepsilon_{\text{bi}}(q, \omega)$ is the determinant of the dielectric tensor,

$$\varepsilon_{\text{bi}}(q, \omega) = \varepsilon_1(q, \omega)\varepsilon_2(q, \omega) - v_{12}^2(q, \omega)\Pi_{11}(q, \omega)\Pi_{22}(q, \omega).$$

The RPA approximates the exact irreducible $\Pi(q, \omega)$ by its simple bubble diagram with respect to the e-e interaction, which, for finite magnetic fields, gives

$$\begin{aligned} \Pi(q, \omega) = & \frac{1}{\pi \ell_B^2} \sum_{l, l'=0}^{\infty} Q_{ll'}(t) \int_{-\infty}^{\infty} \frac{dE}{\pi} f_T(E - E_F) \text{Im} G_l^R(E) \left(\frac{G_{l'}^A(E - \hbar\omega)}{[1 - \delta\gamma_{ll'}^{AA}(t, E, E - \hbar\omega)][1 - \delta\gamma_{ll'}^{RA}(t, E, E - \hbar\omega)]} \right. \\ & \left. + \frac{G_{l'}^R(E + \hbar\omega)}{[1 - \delta\gamma_{ll'}^{AR}(t, E, E + \hbar\omega)][1 - \delta\gamma_{ll'}^{RR}(t, E, E + \hbar\omega)]} \right), \end{aligned} \quad (2)$$

$$\delta\gamma_{ll'}^{ab}(t, E, E \pm \hbar\omega) = \frac{\Gamma_0^2}{4} Q_{ll'}(t) G_l^a(E) G_{l'}^b(E \pm \hbar\omega).$$

For brevity we suppress the layer indices here, and $G_l^{R,A}(E)$ are the electron-retarded and electron-advanced Green's functions, dressed by e - i interaction. In the SCBA they are diagonal and given by $G_l^{R,A}(E) = 2(E - E_l + \sqrt{(E - E_l)^2 - \Gamma_0^2})^{-1}$, with the imaginary part of the square root set to positive (negative) for the advanced (retarded) function. In the short-range impurity model, the half width $\Gamma_0 = \sqrt{(2/\pi)\hbar\omega_B(\hbar/\tau)}$ of the $E_l = (l + 1/2)\hbar\omega_B$ LL is independent of the Landau index l . (τ is the transport relaxation time, determined from mobility μ .) The bare vertex functions $Q_{ll'}(t)$ are given by the gauge-invariant part of the in-plane form factor, $Q_{ll'}(t) = (-1)^{l+l'} e^{-t} L_{l'}^{l-1}(t) L_l^{l'-1}(t)$ where $t = (q\ell_B)^2/2$ and $L_l^l(t)$ is the associated Laguerre polynomial. The denominators in the right-hand side of Eq. (2) differ from one due to the vertex corrections $\delta\gamma_{ll'}^{ab}$, which are obtained consistently in the short-range impurity model with the assumption that the LL are clearly resolved.²¹ The chemical potential $E_F(n, B, T, \mu)$ in the Fermi distribution function f_T is determined implicitly by the electron density via $n = -(2\pi^2\ell_B^2)^{-1} \sum_{l=0}^{\infty} \int_0^{\infty} dE f_T(E - E_F) \text{Im} G_l(E)$. Here we use the electron Green's functions which correspond to the Gaussian density of states, $\text{Im} G_l(E) = \sqrt{2\pi/\Gamma_0} \exp[-2(E - E_l)^2/\Gamma_0^2]$, without unphysical edges of the Landau band.²² We assume spin degeneracy, so the capacity of each LL is doubled.

It is seen in Fig. 1 that $\text{Re} \varepsilon(q, \omega)$ of the individual 2DES becomes negative for intermediate values of ω of the order of Γ_0 [the inverse of Tesla, which equals $\text{m}^2/(\text{V sec})$, is chosen as the unit of mobility]. This requires two crossings of the $\text{Re} \varepsilon(q, \omega) = 0$ axis. The low-frequency zeros (LFZ) of $\text{Re} \varepsilon(q, \omega)$ always lie within the PHC where $\text{Im} \varepsilon(q, \omega)$ is large. The high-frequency zeros (HFZ) are close to or above the upper edge of the PHC where $\text{Im} \varepsilon(q, \omega)$ is small or exactly zero within the SCBA. The pronounced peaks of the dynamical structure factor $S(q, \omega) \propto -\text{Im}[1/\varepsilon(q, \omega)]$, as a function of ω , correspond to the HFZ, while no peaks correspond to the LFZ. Therefore, the HFZ represent the intra-LL CE of the system, while the LFZ cannot be interpreted as

excitations. We believe, however, that these particle-hole states play an important role, particularly in the realization of the frictional magnetodrag effect, and we calculate the LFZ and present them below in the spectrum together with the intra-LL CE modes.

In the bilayer 2DES, there appear a pair of zeros instead of the LFZ and HFZ of the single layer 2DES, and $\text{Re} \varepsilon(q, \omega)$ becomes negative only within small regions, restricted by the two zeros in each pair. Therefore, the bilayer intra-LL CE spectrum consists of two branches which correspond to the in-phase and out-of-phase intra-LL CE. Accordingly, one can see from Fig. 1 that the bilayer structure factor, instead of the single peak of $S(q, \omega)$ of the individual 2DES, shows a double-peak structure near the upper edge of

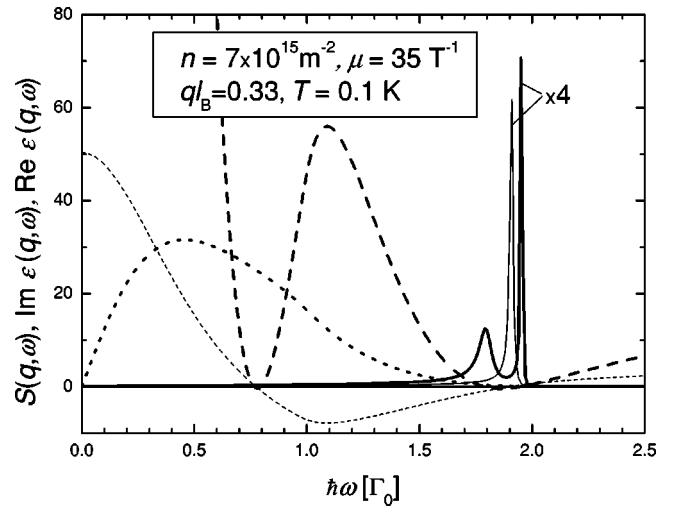


FIG. 1. The structure factor (solid line), the real (dashed line), and the imaginary (dotted line) parts of dielectric function of the bilayer 2DES with the $\Lambda = 30$ nm spacing and for $l_0 = 4$. The thin lines correspond to the individual 2DES, in which $\text{Im} \varepsilon(q, \omega)$ differs from that in the bilayer 2DES by a numerical factor and is not shown here.

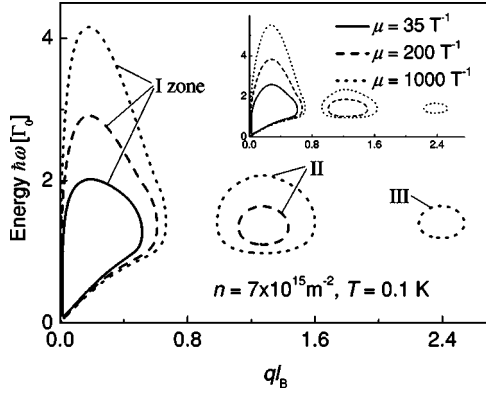


FIG. 2. The dispersion relations of intra-LL CE referred to the $l_0=4$ half-filled LL in the individual 2DES for the three values of mobility. The inset shows the spectra when the LL coupling is not included. It is seen that the wave-vector gaps appear regardless of the inclusion of the LL coupling in the studied regime.

the PHC, while again it demonstrates monotonic behavior at low energies.

In Fig. 2 we plot the spectra of intra-LL CE of individual 2DES at finite temperatures and for various values of electron mobility. The inclusion of the consistent vertex corrections allows us to reproduce the square-root-like dispersion¹⁷ of intra-LL CE at small momenta. However, no exact $q \rightarrow 0$ limit exists in the spectrum. In the *disordered* 2DES the density of states remains finite in the centrum of the LL, and the response function vanishes as q^2 , even if ω is in the immediate vicinity of ω_B . In the short-wavelength limit, again the *disordered* 2DES does not respond, since the response function vanishes exponentially at wavelengths much shorter than ℓ_B . For the lowest $l_0=0$ partially filled LL, there exists only one allowed wave-vector zone [$L_0(t)=1$], and our findings are in agreement with Ref. 17. When a higher LL is partially filled, the number of allowed wave-vector zones can be multiple. As seen from Fig. 2, near half filling of the $l_0=4$ LL and at $T=0.1$ K, there exist only one, two, and three allowed zones for $\mu=35$, 200, and 1000 T^{-1} , respectively, with the wave-vector gaps located around $q\ell_B=0.8$ and 1.87.

A comparison of the spectra obtained neglecting the inter-LL coupling (shown in the inset) with the full outcome indicates that the gaps appearing in the no-coupling case remain the same qualitatively in the weak LL-coupling regime. Also, notice that the formation of the wave-vector gaps is possible only in the disordered 2DES where the density of states is always finite. We find that the size of the gaps decreases when mobility increases and that, due to the divergence of the density of states, the wave-vector gaps cannot survive in the disorder-free case, despite the zeros of the effective e-e interaction. We expect also that the inclusion of the ladder diagrams from the Coulomb correlations will partially smear the zeros of the effective interactions, and instead of the gaps, some structures may be developed in the spectrum.²³

In the first zone close to $q=0$ in Fig. 2, for all three values of μ , the intra-LL CE emerge above the PHC in the middle of the zone where the energy shows a maximum. In this region the spectrum describes CE modes without damping,

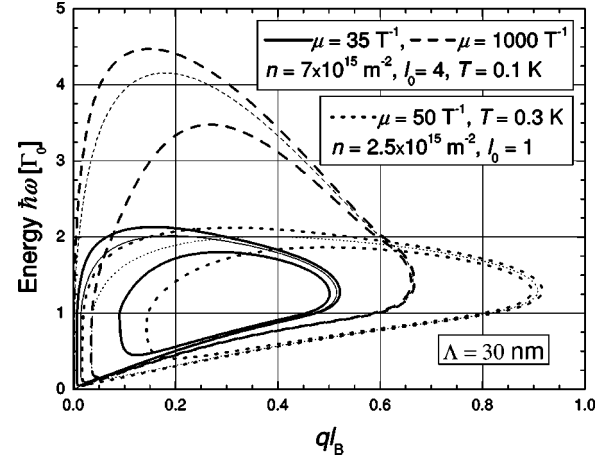


FIG. 3. The dispersion relations of the intra-LL CE in the first allowed wave-vector zone for the bilayer 2DES. The thin lines represent the spectra in the single-layer limit.

and delta-function-like peaks occur in $S(q, \omega)$. Towards the edges of the allowed zone the energy decreases. Within the PHC $\hbar\omega < 2\Gamma_0$, near its upper edge, the peaks of $S(q, \omega)$ become broadened, and though the intra-LL CE modes are damped, there still are well defined excitations. Exactly at the edges of the allowed zone, the group velocity shows anomalous behavior and becomes infinite. At these points CE merge with the particle-hole states, which are described by LFZ of $\text{Re } \varepsilon(q, \omega)$. Below this merging energy the damping is so strong that the zeros of $\text{Re } \varepsilon(q, \omega)$ cannot be interpreted as CE. In the higher zones the energy maximum is smaller and the intra-LL CE emerge above the PHC only in the second zone for the highest value of mobility.

In Fig. 3 we plot the dispersion relations of the intra-LL CE of the bilayer disordered 2DES with the interlayer separation $\Lambda=30$ nm. We restrict our consideration here to the symmetric bilayer 2DES with matched electron densities and present calculations only for the first allowed wave-vector zone. In this case $\varepsilon_1=\varepsilon_2=\varepsilon$, and the bilayer screening function $\varepsilon_{\text{bi}}(q, \omega)$ is represented as

$$\varepsilon_{\text{bi}}(q, \omega) = (1 - \alpha^2)[\varepsilon(q, \omega) - \varepsilon_{\text{in}}(q)][\varepsilon(q, \omega) - \varepsilon_{\text{out}}(q)], \quad (3)$$

where we have defined $\varepsilon_{\text{in,out}}(q) = 1/(1 \pm \alpha^{-1})$ with $\alpha = \exp(-q\Lambda)$. Now the spectrum of the intra-LL CE in the bilayer 2DES is determined implicitly by the conditions $\text{Re } \varepsilon[q, \omega_{\text{in,out}}(q)] = \varepsilon_{\text{in,out}}(q)$.

As seen in Fig. 3, the spectrum of the bilayer intra-LL CE is split into the in-phase and out-of-phase modes. The in-phase CE mode, irrespective of the spacing Λ , is less affected by the interlayer interaction, and lies above it and behaves similarly to the CE mode of individual 2DES. The out-of-phase CE branch lies below the single-layer mode and has a dipole oscillator strength. At small wave vectors the dispersion of in-phase modes is close to the square-root one, while the out-of-phase modes demonstrate a smoother dispersion and achieve the maximum energy at larger values of q . The splitting energy δE decreases in Λ which supports the

tendency that, within the limit of $\Lambda \rightarrow \infty$, the dispersion curves of the in-phase and out-of-phase modes degenerate and coincide with that of the single-layer intra-LL CE mode. δE has a minimum near the upper edge of the PHC and close to the right edge of the allowed wave-vector zone. Towards the right edge of the zone, δE increases slightly, while the increase is strong towards the left edge. The CE modes with q close to the edges of the zone and with energies $\hbar\omega < 2\Gamma_0$ are responsible for the enhancement of the frictional magnetodrag effect. The out-of-phase CE mode has relatively strong damping and contributes largely to the drag effect. However, in certain ranges of wave vectors close to the edges of the allowed zone, the in-phase modes develop and exist solely and will contribute to the drag effect in the absence of the out-of-phase modes.

The corresponding bilayer structure factor for the $l_0=4$ LL is calculated in the plasmon-pole approximation and is depicted in Fig. 1. For $q\ell_B=0.33$ the splitting energy is approximately equal to $0.17\Gamma_0$. For $\mu=35 T^{-1}$ and $B \approx 3.22 T$ we have $\Gamma_0 \approx 4.84$ K, and this gives δE more than 0.8 K. This is a quite measurable quantity; however, notice that at smaller wave vectors, δE is appreciably larger (Fig. 3). As seen from Fig. 1, the out-of-phase peak of $S(q, \omega)$ is about 6 times lower than the in-phase mode peak. However, both the in-phase and out-of-phase CE modes have enough weight to be observed experimentally, and the signatures of these bilayer intra-LL CE in the infrared absorption and inelastic

light-scattering measurements should constitute asymmetric doublets.

We expect that the used approximations are adequate for the 2DES in which disorder dominates over the Coulomb correlations. This is safer in the first allowed zone where $q\ell_B < 1$ and the RPA is an acceptable approximation even in the disorder-free case.¹⁶ In the disordered 2DES, the RPA is valid when no FQHE excitation gap is developed.¹⁷ This is the case if the gap in the disorder-free case Δ_0 is smaller than the typical disorder energy.²⁴ According to Laughlin's estimates²⁵ $\Delta_0 \approx 0.056 E_c$ for the smallest fraction $\nu = \frac{1}{3}$ for which Δ_0 is maximal. Here, we consider the moderate magnetic fields well below the FQHE threshold²⁶ and obtain the intra-LL CE referred to the higher LL. For $\mu=35 T^{-1}$ the ratio E_c/Γ_0 is less than 20, and, near half filling of the $l_0=4$ LL, the system is well away from the regime where FQHE occurs. Thus, we expect that the regime considered here is favorable for the applicability of this theory and for the observation of these novel bilayer intra-LL CEs with attractive many-body and disorder effects.

We thank A. H. MacDonald, S. E. Ulloa, R. Gerhardt, and I. Kukushkin for useful discussions. This work was supported by the Korea Science and Engineering Foundation through Grant No. R05-2003-000-11432-0, by the Ministry of Science and Education of Armenia under Grant No. 0103, and by a DAAD technical grant.

*Permanent address: Radiophysics Department, Yerevan State University, Yerevan 375025 Armenia; Electronic address: badalyan@lx2.yerphi.am

†Electronic address: cskim@boltzmann.chonnam.ac.kr

¹Y. W. Suen, L. W. Engel, M. B. Santos, M. Shayegan, and D. C. Tsui, Phys. Rev. Lett. **68**, 1379 (1992); J. P. Eisenstein, G. S. Boebinger, L. N. Pfeiffer, K. W. West, and Song He, *ibid.* **68**, 1383 (1992).

²A. H. MacDonald, R. Rajaraman, and T. Jungwirth, Phys. Rev. B **60**, 8817 (1999).

³K. Flensberg and B. Y.-K. Hu, Phys. Rev. Lett. **73**, 3572 (1994); Phys. Rev. B **52**, 14 796 (1995).

⁴N. P. R. Hill, J. T. Nicholls, E. H. Linfield, M. Pepper, D. A. Ritchie, G. A. C. Jones, B. Y.-K. Hu, and K. Flensberg, Phys. Rev. Lett. **78**, 2204 (1997).

⁵H. Noh, S. Zelakiewicz, X. G. Feng, T. J. Gramila, L. N. Pfeiffer, and K. W. West, Phys. Rev. B **58**, 12 621 (1998).

⁶M. W. Wu, H. L. Cui, and N. J. M. Horing, Mod. Phys. Lett. B **7**, 279 (1996).

⁷A. V. Khaetskii and Yuli V. Nazarov, Phys. Rev. B **59**, 7551 (1999).

⁸A. Manolescu and B. Tanatar, Physica E (Amsterdam) **13**, 80 (2002).

⁹S. M. Badalyan and C. S. Kim, Solid State Commun. **127**, 521 (2003).

¹⁰R. Z. Vitlina and A. V. Chaplik, Sov. Phys. JETP **54**, 536 (1981); S. Das Sarma and A. Madhukar, Phys. Rev. B **23**, 805 (1981); G. E. Sontoro and G. F. Giuliani, *ibid.* **37**, 937 (1988).

¹¹D. S. Kainth, D. Richards, A. S. Bhatti, H. P. Hughes, M. Y. Simmons, E. H. Linfield, and D. A. Ritchie, Phys. Rev. B **59**, 2095 (1999).

¹²G. R. Aizin and G. Gumbs, Phys. Rev. B **52**, 1890 (1995).

¹³S. V. Tovstonog, L. V. Kulik, I. V. Kukushkin, A. V. Chaplik, J. H. Smet, K. V. Klitzing, D. Schuh, and G. Abstreiter, Phys. Rev. B **66**, 241308(R) (2002).

¹⁴S. M. Girvin, A. H. MacDonald, and P. M. Platzman, Phys. Rev. B **33**, 2481 (1986).

¹⁵S. R. Renn and B. W. Roberts, Phys. Rev. B **48**, 10 926 (1993); A. H. MacDonald and S. C. Zhang, *ibid.* **49**, 17 208 (1994).

¹⁶C. Kallin and B. I. Halperin, Phys. Rev. B **30**, 5655 (1984).

¹⁷D. Antoniou, A. H. MacDonald, and J. C. Swihart, Phys. Rev. B **41**, 5440 (1990).

¹⁸U. Merkt, Phys. Rev. Lett. **76**, 1134 (1996).

¹⁹W. Kohn, Phys. Rev. **123**, 1242 (1961).

²⁰T. Ando, A. Fowler, and F. Stern, Rev. Mod. Phys. **54**, 437 (1982).

²¹M. C. Bønsager, K. Flensberg, B. Y.-K. Hu, and A.-P. Jauho, Phys. Rev. B **56**, 10 314 (1997).

²²R. Gerhardt, Z. Phys. B **21**, 275 (1975); **21**, 285 (1975).

²³L. Brey and H. A. Fertig, Phys. Rev. B **62**, 10 268 (2000).

²⁴A. H. MacDonald, K. L. Liu, S. M. Girvin, and P. M. Platzman, Phys. Rev. B **33**, 4014 (1986).

²⁵R. B. Laughlin, Surf. Sci. **142**, 163 (1985).

²⁶G. S. Boebinger, A. M. Chang, H. L. Stormer, and D. C. Tsui, Phys. Rev. Lett. **55**, 1606 (1985).